

# Quantification of nonuniform distribution of hemi-lung perfusion in chronic obstructive pulmonary disease

Osamu Mitomo<sup>1</sup>

Received: 30 July 2015 / Accepted: 9 November 2015 / Published online: 7 December 2015  
© The Japanese Society of Nuclear Medicine 2015

**Abstract** Nonuniform distribution (NUD) of perfusion on single photon emission computed tomography (SPECT) is caused by impaired perfusion-related fluctuations of the functional volume (FFV). It was determined if digital analysis of NUD in each hemi-lung damaged by chronic obstructive pulmonary disease (COPD) could improve the whole lung impairment assessment. We examined 665 subjects and 8 controls by SPECT. The basic whole lung SPECT volume was defined at 10 % of maximum whole lung count cutoff threshold ( $T_h$ ). For the whole lung and each hemi-lung, the 10 %  $T_h$  width volume, FFV rate, and misfit from the control were calculated at every  $T_h$  width number ( $n$ ) from 1 to 9 for every additional 10 %  $T_h$  from 10 to 100 %. The misfit value integrated from 1 to 9 of  $n$  was defined by 3 NUD indices:  $D$ , whole lung NUD index;  $D_{rl}$ , the index for the sum of each hemi-lung NUD; and  $D^I$ , the NUD index with every interpolating pattern in which FFV rates of hemi-lungs comprised negative and positive value at the same  $n$ .  $D_{rl}$  index was the sum of  $D$  and  $D^I$  indices in all patients.  $D_{rl}$  and  $D$  indices significantly increased in pulmonary disease subjects relative to those of the normal group and non-pulmonary disease subjects.  $D_{rl}$  and  $D$  indices increased in COPD subjects. Progressive COPD subjects had larger  $D_{rl}$  index values and “diffuse and even” hemi-lung impairment. The three indices quantizing FFV itself leading to NUD helped to digitally evaluate the degree of lung impairment of perfusion. Clinically, it is expected that the NUD indices and

images obtained by SPECT, which visually and digitally show the pathological fluctuations in perfusion caused by lung impairment, will be able to provide specific and useful information for improving treatment and/or care of subjects with COPD.

**Keywords** Fluctuation of functional volume · Nonuniform distribution · SPECT · Pulmonary perfusion scintigraphy · COPD

## Introduction

Lung diseases may cause not only reduction or blockage of pulmonary perfusion, which is known as a drop in perfusion, but also a simultaneous rise in perfusion in the unimpaired areas of the lung as a compensatory reaction. Subjective and/or objective symptoms may be manifested as fluctuations in pulmonary perfusion followed by impaired perfusion. <sup>99m</sup>Tc-macroaggregate albumin (99mTc-MAA) pulmonary perfusion scintigraphy has been performed to visually determine if pulmonary perfusion is impaired, and if so, to evaluate the extent of the impaired lung area [1–3]. Scintigrams of subjects with impaired perfusion often show nonuniform distribution (NUD). Furthermore, pulmonary perfusion single photon emission computed tomography (SPECT) can be used to calculate the functional volume of perfusion to assess residual lung function and can provide three-dimensional images of pulmonary perfusion. Quantification of the whole lung NUD by scintigraphy has been used to determine the distribution index of the whole lung ( $D$  index) [4]. However, it is possible that the differences in the NUDs of each hemi-lung have not been accounted for in the  $D$  index. Therefore, in damaged lungs, particularly those damaged by chronic

✉ Osamu Mitomo  
mitomoo@hosp.go.jp

<sup>1</sup> Department of Radiology, National Hospital Organization Numata Hospital, 1551-4 Kamihara-machi, Numata 378-0051, Japan

obstructive pulmonary disease (COPD), we sought to determine if digital analysis of the NUDs of each hemi-lung could improve assessment of whole lung impairment.

## Materials and methods

A total of 665 patients and 8 control subjects underwent a pulmonary perfusion single photon emission computed tomography (SPECT) examination between February 1996 and November 2011. The total number of the SPECT examinations was 954. The control subjects had no symptoms of breathlessness or chest pain, and no abnormal findings were seen on chest X-rays or CT imaging, including SPECT. The institutional review board approved this retrospective study and waived the need to obtain written informed consent.

On the basis of the subjects' complaints and other radiological and physiological examination findings, the subjects were broadly classified into 4 groups: a normal (N) group, pulmonary (P) group, cardiac (C) group, and others group. The N group consisted of clinically normal subjects without any diagnosis of obvious disease even after they had undergone various examinations, including scintigraphy. The P group consisted of subjects with lung diseases such as lung cancer, COPD, and pulmonary thromboembolism. The C group consisted of subjects with heart diseases, including arrhythmia, angina, and cardiac infarction. The patients with complications of cardiac and pulmonary disease were classified into the P group. The others group consisted of subjects who could not be classified into the other 3 groups. The levels of breathlessness of the subjects were assessed according to Performance Status (PS) Scores, and the severity of respiratory symptoms was classified according to the Fletcher-Hugh-Jones' classification [5] and whether oxygen inhalation was introduced (Table 1). 499 of the study participants underwent blood gas analysis (BGA) immediately before or on the same day of the SPECT examination, and 135 underwent spirometry examination within 2 weeks of the SPECT examination.

For the SPECT examination, the subjects were asked to rest in a supine position. Then, 185 MBq of  $^{99m}\text{Tc}$ -MAA (Lungscinti  $^{99m}\text{Tc}$  injectable; Nihon Medi-Physics Co., Tokyo, Japan) was infused into the antecubital vein. Immediately after a dynamic study of the bolus infusion, SPECT was performed. The gamma camera was a two-detector rotating system (MULTISPECT 2; Siemens Medical Solutions USA, Inc. Hoffman Estates, IL). High-resolution collimators were used, and the zoom size was 1.45. A 20 % window width was centered on the  $^{99m}\text{Tc}$  photopeak (140 keV). Pairs of projection images were recorded for 25 s at  $5^\circ$  intervals over  $180^\circ$ , and a total of 72 projections were acquired. Each projection had a matrix size of  $128 \times 128$ . The data were reconstructed using a filtered back projection with a fifth-order Butterworth filter and a cutoff frequency of 0.23 cycles/pixel. No attenuation corrections were made. Tomographic sections with a thickness of 9.93 mm and a pixel size of 3.31 mm were generated in the transverse, sagittal, and coronal planes. The window level limits ranged from 0 to 100 %.

The region of interest (ROI) was set for the whole lung and each hemi-lung, and the volume of the whole lung reconstructed from the SPECT planes at a 10 % cutoff threshold ( $T_h$ ) of the maximum count for the whole lung was defined as the basic perfusion SPECT volume of the whole lung ( $B_w$ ). According to a previous report [4], the  $T_h$  width number ( $n$ ) was defined from 1 to 9 for every additional 10 %  $T_h$  from 10 to 100 %. The NUD index of the ROI of the whole lung, the  $D$  index, was derived by integrating the size of the differences of the functional volume ( $v_n$ ) between the subject and the control from 1 to 9 of  $n$  [4]. And, to calculate the NUD of hemi-lung perfusion, the functional volume ( $v_{sn}$ ) and the functional volume rate ( $r_{sn} = v_{sn}/B_w$ ) were defined adding "s" to designate ROI of each hemi-lung as well as the whole lung;  $w$ , the whole lung;  $r$ , the right hemi-lung;  $l$ , the left hemi-lung. The  $v_{sn}^c$  and  $r_{sn}^c$  were the averages of 8 controls, and 100 times the difference of  $r_{sn}$  and  $r_{sn}^c$  was defined as the fluctuation of the functional volume (FFV) rate ( $f_{sn}$ ). In addition, the absolute value of  $f_{sn}$  was defined as the misfit ( $m_{sn}$ ). An interpolating ( $I$ ) pattern was defined as one in which  $f_{sn}$  of

**Table 1** Definition of level of breathlessness

Level of breathlessness	PS	Severity of respiration symptoms	Oxygen inhalation	No. of patients	COPD
Level 1 (L1)	0–1	I–II	(–)	286	18
Level 2 (L2)	2	III	(–)	124	16
Level 3 (L3)	3–4	IV–V	(+)	249	66
All				659	100

The level of breathlessness was classified according to PS, severity of respiration symptoms, and whether the patient did or did not require oxygen inhalation. Six patients could not be classified according to respiratory symptoms and/or need for oxygen inhalation

the hemi-lungs comprised negative and positive values at the same  $n$ . In the pattern, twice the smaller of the hemi-lung misfit values was defined as the misfit of the  $I$  pattern ( $m'_n$ ). The misfit value integrated from 1 to 9 of  $n$  was defined by 3 indices:  $D$ , the whole lung NUD index;  $D_{rl}$ , the index for the sum of each hemi-lung NUD; and  $D^I$ , the NUD index for every pattern.

$$D = \sum_{n=1}^{n=9} m_{wn}$$

$$D_{rl} = \sum_{n=1}^{n=9} (m_{rn} + m_{ln})$$

$$D^I = \sum_{n=1}^{n=9} m'_n$$

From the above indices, the following equation was mathematically derived.

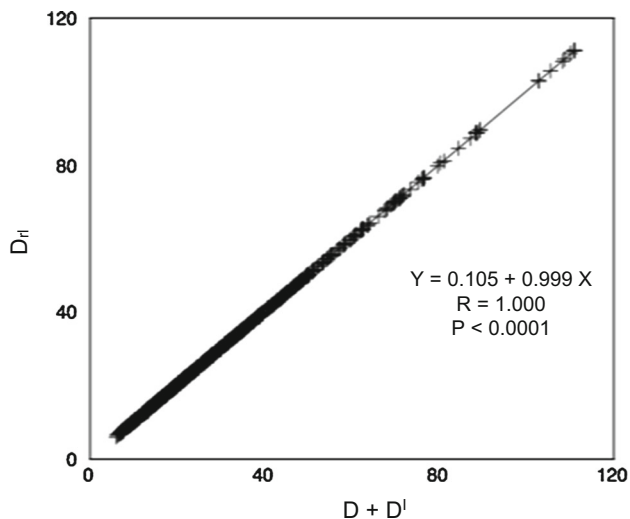


**Fig. 1** The scatter plots of  $D_{rl}$  and the sum of the  $D$  and  $D^I$  indices of the 665 subjects. The significant linear correlation between values of the indices conformed to the mathematical equation ( $D_{rl} = D + D^I$ )

$$D_{rl} = D + D^I$$

Comparisons between groups were performed by using an unpaired Student’s  $t$  test with  $P < 0.05$  taken to indicate significant differences. Single regression analysis was performed between two variables, and the correlation coefficient was determined, with  $P < 0.05$  indicating a significant difference. The statistical analyses were performed with StatView, version 5.0 (SAS Institute, Cary, NC).

**Results**

The  $D_{rl}$  value was linearly correlated with the sum of the  $D$  and  $D^I$  values according to the above equation for the 3 indices (Fig. 1). The  $D_{rl}$  and  $D$  values of the P group were significantly higher than those of the N, C, and others groups (Table 2). In addition, the subjects with COPD showed significant increases in the  $D_{rl}$  and  $D$  indices relative to those of the non-pulmonary group (Fig. 2). Furthermore, the  $D_{rl}$  index of the subjects with COPD significantly increased more in the highly progressive (HP) group than in the slowly progressive (SP) group (Table 3).

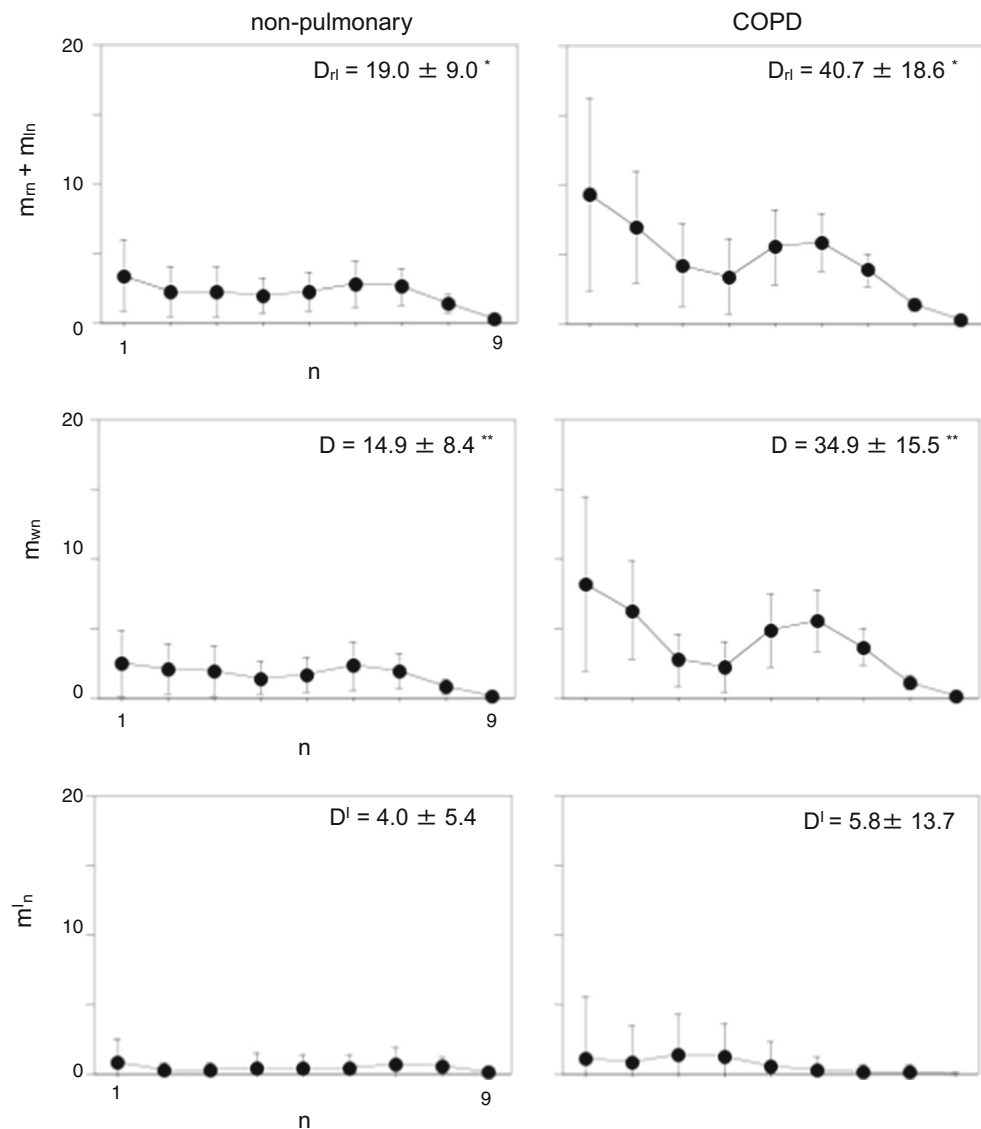
**Discussion**

Various diseases can cause impairments in the lung, and a drop in perfusion in the impaired areas might lead to fluctuations in pulmonary perfusion in the ipsilateral hemi-lung or whole lung. In addition, one of the symptoms of impairment is dyspnea. Examinations for impairment of the lung include morphological imaging, such as chest X-ray and CT examinations, and physiological and functional studies, such as electrocardiography, BGA, and spirometry. Pulmonary scintigraphy is performed to determine if the impairment has a vascular cause [1–3]. When vascular impairment is observed after performing pulmonary perfusion scintigraphy, the

**Table 2** Indices of the subjects in each group

Group	No. of patients	$D_{rl}$ index	$D$ index	$D^I$ index
All	665	31.0 ± 19.3	22.9 ± 13.6	8.0 ± 15.3
N	10	13.3 ± 3.5*, **	11.4 ± 4.2*	1.8 ± 2.0
P	555	33.4 ± 19.9*, ***, ****	24.5 ± 13.9*, ***, ****	8.8 ± 16.4
C	53	19.7 ± 8.9****, **	14.3 ± 7.5****	5.3 ± 6.6
Others	47	19.3 ± 9.6****	16.2 ± 9.7**	3.0 ± 3.9
$P$ value		* $P < 0.005$ ** $P < 0.05$ ***, **** $P < 0.0001$	* $P < 0.005$ ***, **** $P < 0.0001$	

**Fig. 2** Misfit curves of the 3 indices for subjects with non-pulmonary disease and COPD. The value of misfit integrated from 1 to 9 of  $n$  was defined as the NUD index, and the means and standard deviations of each index of each group are shown. \*, \*\* $P < 0.0001$



scintigram, which is an image showing the accumulation and distribution of  $^{99m}\text{Tc}$ -MAA particles in pulmonary perfusion, shows defects or shaded areas that reflect the NUD of  $^{99m}\text{Tc}$ -MAA particles. The NUD is itself a three-dimensional expression of FFV that is caused by both a drop in perfusion in the impaired area and a rise in perfusion in the other areas of the lung. Pulmonary perfusion scintigraphy SPECT can analyze the FFV precisely by allowing integration of the decrease and increase in perfusion at every threshold width in the process of three-dimensional reconstruction. On the other hand, the distribution index of the lung as a whole ( $D$  index) [4] is not an indicator of the NUD of each hemi-lung but rather of the whole lung. Therefore, to quantitate the NUD of each hemi-lung,  $D$  indices were calculated for each hemi-lung by setting ROI in each

hemi-lung. The FFV rate was the difference between the subject and control and was indicated by the negative value for the decrease or the positive value for the increase, and the magnitude of each FFV at every 10 % cutoff  $T_h$  width number ( $n$ ) from 1 to 9 was defined as the misfit, and the total amount of every misfit was calculated using the indices of the NUDs for the whole lung, hemi-lungs, and between the hemi-lungs. In all 665 patients, the  $D_{rl}$  was the sum of the  $D$  and  $D^l$  indices (Fig. 1), which suggested that the sum of the NUDs of the two hemi-lungs was not the NUD of the whole lung except when the  $D^l$  index is zero. The  $D_{rl}$  and  $D$  indices of the P group were significantly higher than those of the N, C, and others groups (Table 2). The  $D_{rl}$  and  $D$  indices of the subjects with COPD significantly increased relative to those of the non-pulmonary group (Fig. 2). It was

**Table 3** Spirometric, blood gas analysis, and SPECT results for the slowly and highly progressive COPD groups classified by the level of breathlessness

Disease	COPD		P value
Group classified by degree of progression	SP	HP	
Levels of breathlessness	L1 and L2	L3	
No. of subjects	34	66	
Clinical results of spirometry and BGA			
%VC	85.1 ± 19.2 (21)	65.0 ± 14.4 (28)	0.0001
FEV1 %	73.5 ± 25.4 (21)	58.1 ± 19.1 (28)	0.0189
%FEV1	76.9 ± 16.6 (15)	32.8 ± 8.6 (7)	<0.0001
pO <sub>2</sub> /FiO <sub>2</sub>	354.2 ± 52.2 (22)	275.8 ± 70.8 (48)	<0.0001
Values of the indices calculated by the SPECT			
$D_{rl}$ index	33.8 ± 15.7 (34)	44.3 ± 19.0 (66)	0.0066
$D$ index	30.8 ± 16.0 (34)	37.0 ± 15.0 (66)	0.0548
$D^I$ index	2.9 ± 4.3 (34)	7.2 ± 16.4 (66)	0.1368

The number of subjects is shown in parentheses

SP and HP slowly and highly progressive groups, respectively, SPECT single photon emission computed tomography, COPD chronic obstructive pulmonary disease, %VC the predicted vital capacity, FEV1% the forced expiratory volume in one second (FEV1) to forced vital capacity, %FEV1 FEV1 % predicted, pO<sub>2</sub>/FiO<sub>2</sub> the ratio of arterial oxygen partial pressure to fractional inspired oxygen

thought that the increase in the  $D_{rl}$  and  $D$  indices would be helpful to digitally determine if a patient had pulmonary impairment. To determine if the index of the NUD could be used to evaluate deterioration caused by COPD, the subjects with COPD were classified into 2 groups according to the level of breathlessness (Table 1). There were significant differences in the spirometric and BGA results between the 2 groups (Table 3), and it was thought that the respiratory condition of the HP group would be greater than or equal to the stage III in the Global Initiative for Chronic Obstructive Lung Disease (GOLD 3) [6] or near respiratory failure [7]. In a concrete case (Fig. 3; Table 4), the NUD indices digitally demonstrated the severity of the COPD and the improvement of the impairment in the pulmonary perfusion about 3 years later. The HP group also had a significantly greater increase in the  $D_{rl}$  index than that of the SP group, without showing an increase in the  $D^I$  index. It should be noted that the  $D^I$  index allows the  $D_{rl}$  index to increase by adding the misfit in the hemi-lungs and the  $D$  index to decrease by interpolating the FFV rate between the hemi-lungs. The relationship between the  $D$  and  $D^I$  indices was typically observed in the subjects with a large imbalance in perfusion between the hemi-lungs, specifically in the subjects with advanced lung cancer (LC), similar to the case in Fig. 4. In the advanced LC subjects in whom the primary tumor was larger and/or showed invasion into the ipsilateral hilum,

much greater increases in the  $D^I$  index than those in the non-advanced LC subjects were observed, without increases in the  $D$  index (Table 5). On the other hand, the average FFV rate curve of the whole lung of the COPD subjects showed that the size of the  $D$  index was generally related to the drop in perfusion of the more highly functioning volumes of  $\geq 40$  % of the cutoff  $T_h$  in the whole lung (Fig. 5). From the above, it was speculated that greater deterioration caused by COPD led to a greater increase in  $D_{rl}$ , which was related to both the increase in the NUDs of the “diffuse and even” impairments of the hemi-lungs and the fundamental background of the decrease in the more highly functional volume of  $\geq 40$  % of the cutoff  $T_h$ ; in other words, the increase in the less functional volume of  $< 40$  % of the cutoff  $T_h$  of the whole lung. Endothelial dysfunction and vascular remodeling in the pulmonary vascular bed have been observed in COPD [8]. It is speculated that the vascular remodeling is induced as a result of the interrelation between a drop in perfusion in the impaired area and a rise in perfusion in the other areas of the lung, observed as the NUD on the scintigram. And it is thought that rather than evaluating impairment of the bronchial airway in COPD [9, 10], digital assessment of the NUD of 99mTc-MAA particles in scintigraphy can be used to show the degree of the vascular impairment or remodeling of the COPD because the pulmonary vessels and bronchial airways are reciprocally related in

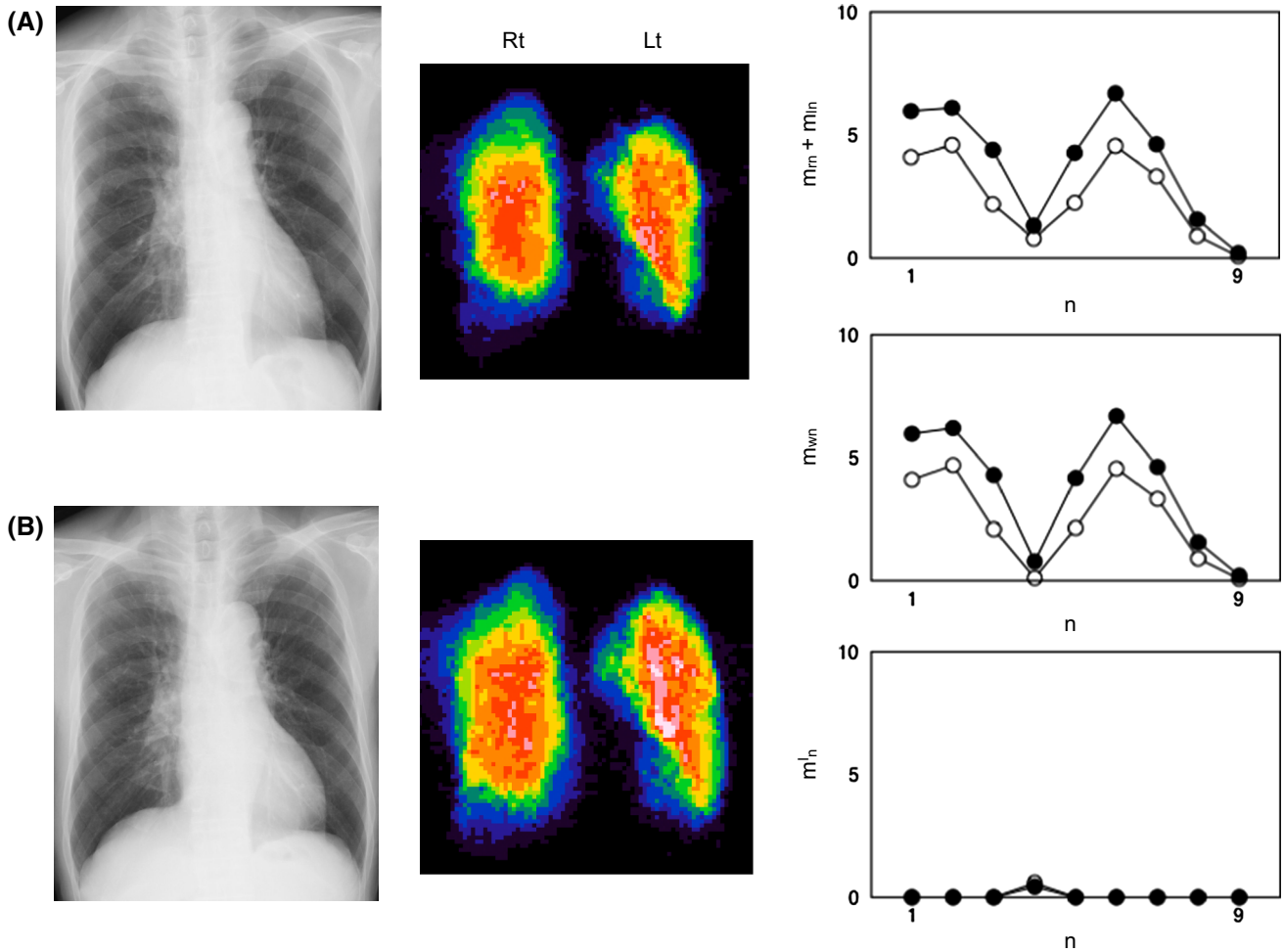


**Fig. 3** Chest X-ray, reconstructed three-dimensional (3D) frontal view SPECT images, and misfit curves of the 3 indices of a patient of HP group with COPD at the first time examination (a) and those at the reexamination (b). The filled and open circles showed the misfit

curves of the 3 indices at a and b, respectively. The clinical data and the NUD indices were shown in Table 4. Rt and Lt represent the right, and left hemi-lung, respectively

**Table 4** A concrete case of HP group with COPD

SPECT examination	Age (year)	PS	Severity of respiration symptoms	Oxygen inhalation	%VC	FEV1 %	%FEV1	pO <sub>2</sub> /FiO <sub>2</sub>	D <sub>rl</sub>	D	D <sup>f</sup>
1st	83	1	IV	(-)	72.9	41.7	36.4	411.9	35.1	34.5	0.4
2nd	86	1	IV	(-)	89.0	47.4	41.5	384.8	22.8	22.0	0.6

The first SPECT examination had let the male subject be orally prescribed a prostaglandin I2 analog. The second examination demonstrated the improvement of the NUD indices as well as no deteriorations of the other clinical findings, and he passed away 3 years later

function in the lung. On the other hand, fluctuations in pulmonary perfusion are also influenced by the structure and function of the bronchovascular tree [11], gravity [12], the function of capillaries surrounding the alveoli [13], cardiac function [14], nervous and muscular function [15, 16], humoral modulators or mediators [17, 18],

and other factors [19]. In addition, it is thought that the FFV should be comprehensively estimated by accounting for the interactions of the various factors. However, it is considered that the FFV is the evidence letting both the medical expert and the patient know the event in which some vascular impairment arose in the bronchovascular



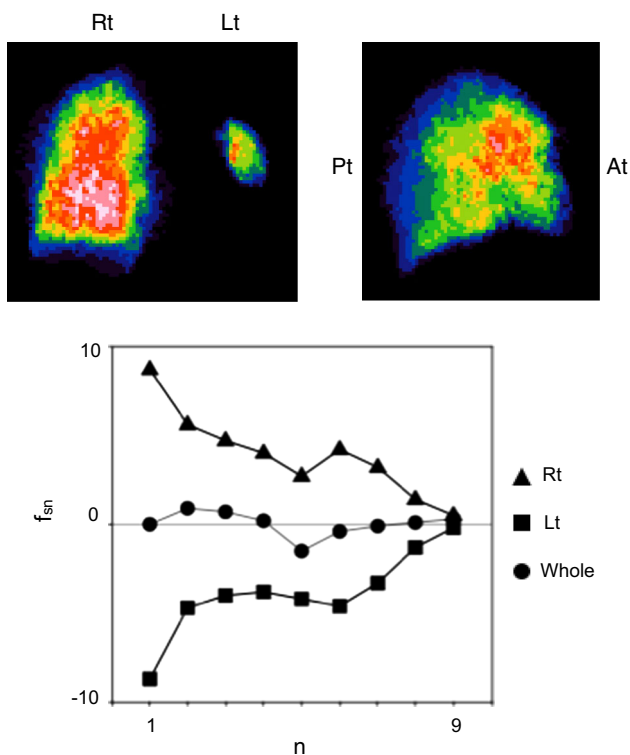


**Fig. 4** 3D frontal and lateral view SPECT images of a lung cancer patient with the invasion by the primary tumor of the left hilum (T4N0M0). The FFV rate curves at every  $n$  were presented for the whole lung and hemi-lung; the  $D$ ,  $D_{Rt}$ , and  $D^l$  indices were 3.9, 69.8, and 65.7, respectively. The imbalance in perfusion between the hemi-lungs specifically showed the interpolating pattern at every  $n$ , and the  $D^l$  index showed the large size, but the  $D$  index was almost normal.  $Rt$ ,  $Lt$ ,  $At$ ,  $Pt$ , and  $whole$  represent the right, the left hemi-lung, anterior, posterior, and the whole lung, respectively

**Table 5** The values of the indices for the non-advanced and advanced LC groups

Disease	LC		<i>P</i> value
T and N factors	≤T2a and N0	≥T2b and/or ≥N1	
No. of subjects	52	120	
Values of the indices			
$D_{Rt}$ index	23.4 ± 10.4	38.5 ± 24.1	<0.0001
$D$ index	20.2 ± 10.9	21.4 ± 10.5	0.482
$D^l$ index	3.2 ± 4.3	17.1 ± 24.0	<0.0001

T and N were classified by the 7th Union International Cancer Control TNM classification of malignant tumors

tree of the lung being followed by a variation of vascular volume. Clinically, it is expected that the NUD indices and images obtained by SPECT, which visually and digitally show the pathological fluctuations in perfusion caused by lung impairment, can provide specific and useful information for improving treatment and/or care

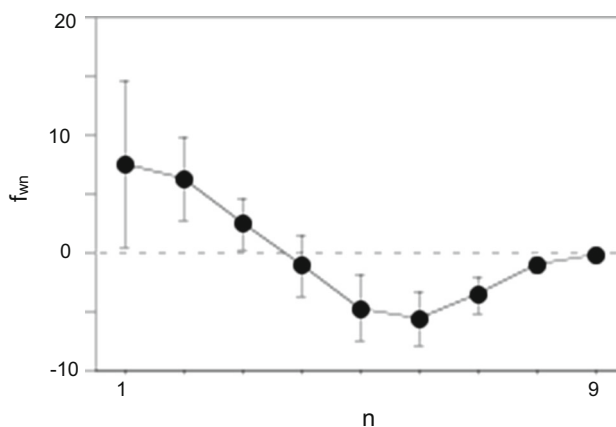


**Fig. 5** The averaged whole lung FFV rate ( $f_{wn}$ ) curve of COPD subjects. The decrease in the more highly functioning volume and the increase in the less functioning volume were demonstrated at the 40 % cutoff  $T_h$ . There were significant differences in the means of  $f_{wn}$  among the  $n$  except between 4 and 8 of  $n$  and between 1 and 2 of  $n$

of subjects with COPD, being compared with or referred to other quantitative imaging approaches such as CT and MRI that are making rapid progress [20].

**Acknowledgments** The author thanks the staff of the Department of Radiology, Dr. Hidemasa Kuwabara, Dr. Katsuya Kato (General Ota Hospital, Ota, Japan), Dr. Kiyokazu Arai and the members of the staff in the Advanced Medical Imaging and Analysis Center (AMIAC, Maebashi, Japan), and Dr. Takayuki Kohri (Tone Chuou Hospital, Numata, Japan) for the examinations. I also thank the staff of Siemens Japan, MI Business Management Dept., for technical assistance during quantification of image data. In addition, I would like to thank Enago (<http://www.enago.jp>) for the English language review.

**Compliance with ethical standards**

**Conflict of interest** The author has no conflicts of interest.

**References**

- Carratu L, Salvatore M, Lopez-Majano V, Sofia M, Muto P, Ariemma G. Single photon emission computed tomography study of human pulmonary perfusion: preliminary findings. Nucl Med Commun. 1984;5:91–9.
- Petersson J, Sánchez-Crespo A, Larsson SA, Mure M. Physiological imaging of the lung: single-photon-emission computed tomography (SPECT). J Appl Physiol. 2007;102:468–76.
- Sostman HD, Miniati M, Gottschalk A, Matta F, Stein PD, Pistolesi M. Sensitivity and specificity of perfusion scintigraphy combined with chest radiography for acute pulmonary embolism in PIOPED II. J Nucl Med. 2008;49:1741–8.
- Mitomo O, Aoki S, Tsunoda T, Yamaguchi M, Kuwabara H. Quantitative analysis of nonuniform distributions in lung perfusion scintigraphy. J Nucl Med. 1998;39:1630–5.
- Fletcher CM. The clinical diagnosis of pulmonary emphysema; an experimental study. Proc R Soc Med. 1952;45:577–84.
- Global Initiative for Chronic Obstructive Lung Disease (GOLD). Global strategy for the diagnosis, management, and prevention of chronic obstructive pulmonary disease (COPD). 2015. <http://>

- [www.goldcopd.org/guidelines-global-strategy-for-diagnosis-management.html](http://www.goldcopd.org/guidelines-global-strategy-for-diagnosis-management.html). Accessed 24 Apr 2015.
7. Kawakami Y, Irie T, Kishi F. Criteria for pulmonary and respiratory failure in COPD patients—a theoretical study based on clinical data. *Respiration*. 1982;43:436–43.
  8. Wright JL, Levy RD, Churg A. Pulmonary hypertension in chronic obstructive pulmonary disease: current theories of pathogenesis and their implications for treatment. *Thorax*. 2005;60:605–9.
  9. Mets OM, de Jong PA, van Ginneken B, Gietema HA, Lammers JW. Quantitative computed tomography in COPD: possibilities and limitations. *Lung*. 2012;190:133–45.
  10. Bajc M, Markstad H, Jarenbäck L, Tufvesson E, Bjermer L, Jögi J. Grading obstructive lung disease using tomographic pulmonary scintigraphy in patients with chronic obstructive pulmonary disease (COPD) and long-term smokers. *Ann Nucl Med*. 2015;29:91–9.
  11. Glenny RW, Lamm WJ, Bernard SL, An D, Chornuk M, Pool SL, et al. Selected contribution: redistribution of pulmonary perfusion during weightlessness and increased gravity. *J Appl Physiol*. 2000;89:1239–48.
  12. West JB. Regional differences in the lung. *Chest*. 1978;74:426–37.
  13. Baumgartner WA Jr, Jaryszak EM, Peterson AJ, Presson RG Jr, Wagner WW Jr. Heterogeneous capillary recruitment among adjoining alveoli. *J Appl Physiol*. 2003;95:469–76.
  14. Han MK, McLaughlin VV, Criner GJ, Martinez FJ. Pulmonary diseases and the heart. *Circulation*. 2007;116:2992–3005.
  15. Ingram RH, Szidon JP, Skalak R, Fishman AP. Effects of sympathetic nerve stimulation on the pulmonary arterial tree of the isolated lobe perfused in situ. *Circ Res*. 1968;22:801–15.
  16. Qureshi A. Diaphragm paralysis. *Semin Respir Crit Care Med*. 2009;30:315–20.
  17. Esteve JM, Launay JM, Kellermann O, Maroteaux L. Functions of serotonin in hypoxic pulmonary vascular remodeling. *Cell Biochem Biophys*. 2007;47:33–44.
  18. Palmer RM, Ferrige AG, Moncada S. Nitric oxide release accounts for the biological activity of endothelium-derived relaxing factor. *Nature*. 1987;327:524–6.
  19. Hsia CC. Signals and mechanisms of compensatory lung growth. *J Appl Physiol*. 2004;97:1992–8.
  20. Hopkins SR, Wielpütz MO, Kauczor HU. Imaging lung perfusion. *J Appl Physiol*. 2012;113:328–39.